OXFORD

ORIGINAL ARTICLE

18β-glycyrrhetinic acid inhibited mitochondrial energy metabolism and gastric carcinogenesis through methylation-regulated TLR2 signaling pathway

Donghui Cao[1], Yanhua Wu[1], Zhifang Jia[1], Dan Zhao[1], Yangyu Zhang[1], Tianyu Zhou[2], Menghui Wu[2], Houjun Zhang[2], Tetsuya Tsukamoto[3], Masanobu Oshima[4], Jing Jiang[1] and Xueyuan Cao[2,*,◉]

[1]Division of Clinical Research and [2]Department of Gastric and Colorectal Surgery, First Hospital of Jilin University, Changchun, Jilin 130021, China, [3]Department of Diagnostic Pathology I, School of Medicine, Fujita Health University, Toyoake 470–1192, Japan and [4]Division of Genetics, Cancer Research Institute, Kanazawa University, Kanazawa 920–1192, Japan

*To whom correspondence should be addressed. Tel: +86 431 81875609; Fax: +86 431 88782889; Email: caoxy@aliyun.com
Correspondence may also be addressed to Jing Jiang. Tel: +86 431 81875408; Fax: +86 431 88782889; Email: jiangjing19702000@jlu.edu.cn

Abstract

The natural phenolic substance, 18β-glycyrrhetinic acid (GRA), has shown enormous potential in the chemoprevention of cancers with rich resources and biological safety, but the GRA-regulated genetic and epigenetic profiles are unclear. Deregulated mitochondrial cellular energetics supporting higher adenosine triphosphate provisions relative to the uncontrolled proliferation of cancer cells is a cancer hallmark. The Toll-like receptor 2 (TLR2) signaling pathway has emerged as a key molecular component in gastric cancer (GC) cell proliferation and epithelial homeostasis. However, whether TLR2 influenced GC cell energy metabolism and whether the inhibition effects of GRA on GC relied on TLR2 signaling were not illustrated. In the present study, TLR2 mRNA and protein expression levels were elevated in gastric tumors in the K19-Wnt1/C2mE (Gan) mice model, GC cell lines and human GCs, and the overexpression of TLR2 was correlated with the high histological grade and was a poor prognostic factor in GC patients. Further gain and loss of function showed that TLR2 activation induced GC cell proliferation and promoted reactive oxygen species (ROS) generation, Ca^{2+} accumulation, oxidative phosphorylation and the electron transport chain, while blocking TLR2 inhibited mitochondrial function and energy metabolism. Furthermore, GRA pretreatment inhibited TLR2-activated GC cell proliferation, energy metabolism and carcinogenesis. In addition, expression of TLR2 was found to be downregulated by GRA through methylation regulation. Collectively, the results demonstrated that GRA inhibited gastric tumorigenesis through TLR2-accelerated energy metabolism, suggesting GRA as a promising therapeutic agency targeting TLR2 signaling in GC.

Introduction

Gastric cancer (GC) is one of the most common malignancies; statistics from the Union for International Cancer Control (UICC) show that 951 000 new cases and 723 000 deaths of GC occurred in 2012 worldwide, accounting for fifth in occurrence and third in death of all malignant tumors (1). In China, the report from Cancer Registration showed that ~427 000 new cases and 301 000 deaths of GC occurred in 2013, and it estimated that the morbidity and mortality of GC in 2015 were ranked second only to lung cancer (2). GC has become a serious public health problem; thus, to explore the early intervention and chemoprevention therapy of GC, reducing the incidence of GC is imperative.

Abbreviations

ATP	adenosine triphosphate
ETC	electron transport chain
GC	gastric cancer
GRA	glycyrrhetinic acid
OXPHOS	oxidative phosphorylation
PA-LPS	Pseudomonas aeruginosa lipopolysaccharide
PBS	phosphate-buffered saline
TLR2	toll-like receptor 2.

18β-glycyrrhetinic acid (GRA) is present in the roots of *Glycyrrhiza glabra* L. Our previous studies have found that GRA possesses pharmacological actions, such as anti-inflammatory and antitumor effects (3,4). Although various genes and pathways, such as canonical Wnt, PGE2-EP2, reactive oxygen species (ROS)/PKC-α/ERK pathways, were shown to be potential targets of GRA (3,5,6), the systematic research on GRA-regulated genetic and epigenetic profiles was not studied sufficiently.

Toll-like receptor (TLR) family is an essential subset of pathogen recognition receptors, which are key regulators of innate and adaptive immune responses and recognize pathogenic microbes in chronic inflammation and carcinogenesis. It has been shown that TLR 2 signal can be induced by *Helicobacter pylori*, and its activation promotes the secretion of inflammatory cytokines and plays a key role in GC tumorigenesis (7). Importantly, an ever-increasing amount of data has shown that the TLR2 signal through MyD88, which leads to the activation of NF-κB, PI3K/Akt as well as p38, ERK and c-Jun MAPK pathways, is important for epithelial homeostasis and tumorigenesis. Notably, disruption of the TLR2 gene (*Tlr2*) in GC mouse model $gp130^{F/F}$ resulted in the significant suppression of tumor formation (8). DNA microarray-based expression profiling demonstrated that the TLR2-induced growth responsiveness of human GC cells corresponded with some antiapoptotic and tumor suppressor genes (9).

Meanwhile, the TLR family is closely associated with mitochondrial energy metabolism. The uncontrolled cell proliferation that represents the essence of neoplastic disease demands higher adenosine triphosphate (ATP) provisions compared with non-cancer cells and altered mitochondrial bioenergetics, a major source of ATP, which might underlie the development of cancer (10). TLR9 sensed hypoxia conditions, induced p38-MAPK signaling pathway and then activated mitochondrial biogenesis and promoted cancer cell survival (11). TLR4 induced ROS production, increased mitochondrial membrane potential and promoted GC progression (12). West *et al.* indicated that increased TLR2 gene expression augmented GC cell growth (9); however, until now, whether TLR2 was associated with mitochondrial bioenergetics in GC has not been reported.

There is considerable evidence suggesting that targeting energy metabolism appears to be a promising strategy to inhibit carcinogenesis and development. The well-known cancer chemopreventive phytochemicals, phenethyl isothiocyanate extract from watercress, benzyl isothiocyanate from garden cress and sulforaphane from broccoli have been shown to inhibit the electron transport chain (ETC) and induce generation of ROS (13). Although some researchers have shown that GRA modulated mitochondrial function, decreased cytochrome C release and induced cancer cell apoptosis (14), the possible effects of GRA on energy metabolism and mitochondrial bioenergetics have not been well studied.

In the present study, the whole transcriptome gene expression changed after GRA treatment was measured. GRA pretreatment downregulated the TLR2 signaling pathway, while its overexpression promoted mitochondrial energy metabolism, ROS generation, GC cell proliferation and GC tumorigenesis. The collective results suggested that GRA was a promising pretreatment and therapeutic agency in GC.

Material and methods

GC cell lines

The human gastric tumor cell lines HGC-27, MKN-1, AGS and KATOIII, as well as the immortal gastric epithelia cell lines GES-1, were maintained in Roswell Park Memorial Institute 1640 or DMEM media (HyClone, Logan, UT) containing 10% heat-inactivated FBS (Gibco, New York), penicillin (100 U/ml) and streptomycin (100 U/ml) (HyClone). The cells were incubated in humidified air with 5% CO_2 at 37°C and subcultured with 0.25% trypsin and 0.02% ethylenediaminetetraacetic acid.

Authentication of cell lines

All the GC cell lines were purchased from Cobioer company (Nanjing, China), and they were tested and authenticated by Genetic testing biotechnology company (Suzhou, China) in 29 June 2018. Cell lines were authenticated using short tandem repeat analysis as described in 2012 in ANSI Standard (ASN-0002) by the ATCC Standards Development Organization (SDO) and in Capes-Davis's paper (15).

Transgenic animal model and 18β-GRA administration

K19-Wnt1/C2mE (Gan) mice were constructed by the Oshima group with simultaneous activation of Wnt signaling and the COX-2/PGE2 pathway (16). Gan mice were obtained from the Cancer Research Institute (Kanazawa, Japan) and housed in pathogen-free conditions. The detailed breeding conditions were used as described previously (17).

Gan mice aged 6 weeks old were randomly assigned to two groups: Control group (*n* = 36) and GRA-treated group (*n* = 36). 18β-GRA (Sigma, St. Louis, MO) was dissolved in distilled water at 0.05% (mass concentration) for *in vivo* study. This solution was freshly prepared three times per week and administered as drinking water. Control mice were fed with the same diet and distilled water but without GRA. For *in vitro* study, the concentration of GRA was 50–200 μM. The dose and usage of GRA were chosen based on our previous study (3). The mice were killed 48 weeks after GRA administration. All animals were subjected to deep ether anesthesia. The whole stomach was excised from each animal and washed in cold phosphate-buffered saline (PBS). Tumor size was recorded. All samples were separated into two parts: one part was paraffin-embedded for hematoxylin-eosin (HE) and immunohistochemistry (IHC) staining, and the other part was fresh-frozen in liquid nitrogen and preserved at –80°C until DNA, RNA and protein extraction.

Human GCs

Fifty-three cases of GC were collected from the patients in the First Hospital of Jilin University who underwent operation between September 2008 and January 2012. The GC and paired control tissues were obtained. The median follow-up time for the patients was 21.3 months (from 1.5 to 59.1 months).

Ethics statement

All procedures involving the use of samples from animals and patients were carried out with prior approval from the Institutional Research Ethics Committee of Jilin University (Changchun, China). Informed consent was obtained from all patients involved in the study.

HE and immunohistochemistry staining

Paraffin-embedded GC tissues from Gan mice and humans were prepared. HE staining and immunohistochemistry staining of TLR2 (polyclonal, PRS3135, Sigma), Ki-67 (polyclonal, ab15580, Abcam, Cambridge), F4/80 (monoclonal, clone no. BM8, ab16911, Abcam) were carried out in a humidified chamber. The immunohistochemistry staining of TLR2, Ki-67, F4/80 in mice gastric tumors was analyzed using H score system as described previously (17). As in brief, the percent of stained tumor cells

was recorded in 5% increments from a range of 0–100 (P0, P1–3), and the staining intensity was scored from 0 to 3 [I0 (normal), I1 (mild), I2 (moderate) and I3 (marked)], and H score (range 0–300) was obtained by adding the sum of individual scores obtained for each tissue (H score = I1 × P1 + I2 × P2 + I3 × P3).

Evaluation of expression of TLR2 protein expression

TLR2 protein expression was predominantly observed in the cell membrane and cytoplasm. The immunoreactive scores of Remmele and Stegner (IRS) system was used to assess the staining intensity and percentages of the tumor cells. The intensity was subdivided into four categories: 0 (no immunostaining), 1 (weak), 2 (moderate) or 3 (strong), and the percentages were subdivided into five grades: 0 (<1% expression), 1 (1–10% expression), 2 (11–30% expression), 3 (31–60% expression) and 4 (≥61% expression). The product of intensities and percentages resulted in an IRS value ranging from 0 to 12. A total score of <5 was defined as weak, 5–9 was defined as moderate and >9 was defined as strong expression.

Agonist and inhibitor treatments

For the TLR2 stimulating experiments, GC cells were treated with specific TLR2 agonist *Pseudomonas aeruginosa* lipopolysaccharide (PA-LPS) (18) (Sigma). For TLR2 blocking experiments, GC cells were treated with the specific TLR2 inhibitor CU CPT 22 (Tocris Bioscience, Bristol, UK) (19).

Cell viability and proliferation assay

The cell viability was calculated using an MTT assay (Promega, Shanghai, China), the cell proliferation was measured using colony formation assay and all procedures were used as reported previously (3).

Wound healing

A total of 5×10^5 cells were plated in 6-well plates. Scratches were created using a 10 µl pipette tip. Then, the progression of migration was examined and photographed after 72 h by a microscope (400× amplification, Olympus, Japan).

Western blot

The total protein was collected from GC tissues, and GC cells homogenized in strong RIPA buffer (Kangwei, China), containing a protease inhibitor and phosphatase inhibitor (Kangwei). The protein concentration was determined by a BCA protein assay kit (Kangwei). The levels of TLR2 (1:2000, Sigma), TLR4 (1:1000, Abcam), COX-2 (1:1000, Santa Cruz, CA), NF-κB, MyD88, Wnt-1, β-catenin and GAPDH (1:1000, Abcam) were visualized using an ECL kit (Pierce, Rockford). The signals were observed using an Imaging System (Tanon, China).

Intracellular ROS assay

The changes of ROS in GC cell lines were observed with the molecular probe DCFH-DA (Beyotime, China). After treatment, the cells were incubated with DCFH-DA diluted in 1:1000 with fresh medium for 30 min at 37°C, and cells were washed with PBS to remove excess DCFH-DA. The cells were analyzed by a microplate reader (Biotek) for fluorescence excited at 488 nm and emitted at 525 nm.

Measurement of mitochondrial transmembrane potential

The changes in mitochondrial transmembrane potential (ΔΨm) in the GC cell lines were observed with JC-1 fluorescent probes (Beyotime) by a microplate reader (Biotek). After treatment, cells were labeled with JC-1 (2.5 mg/ml) for 20 min at 37°C; then, cells were washed with PBS to remove excess JC-1. The monomer of JC-1 was analyzed for fluorescence on a microplate reader excited at 490 nm and emitted at 530 nm, while the aggregates of JC-1 were analyzed using 525 nm excitation with 590 nm emission filters.

Ca²⁺ level assay

The changes of the Ca^{2+} level in GC cell lines were observed with a molecular probe Fluo-4 AM (Beyotime). After treatment, cells were incubated with Fluo-4 AM diluted in 1:1000 with fresh medium for 30 min at 37°C;

then, cells were washed with PBS to remove excess Fluo-4 AM. The cells were analyzed by a microplate reader (Biotek) for fluorescence excited at 488 nm and emitted at 520 nm.

Oxygen consumption rate (OCR) measurement

Multiple parameters of mitochondrial function, including basal OCR, spare respiratory capacity, maximal OCR, ATP-linked respiration and proton that leaked from adherent intact cultured cells, were measured using a Seahorse XF96 Extracellular Flux Analyzer (Seahorse Bioscience, Billerica, MA). After baseline measurements, OCR was measured after sequentially adding 1 mg/ml oligomycin, 1 mM FCCP and 1 mM rotenone to each well. All assays were conducted using a seeding density of 10 000 cells/well in 200 ml of Roswell Park Memorial Institute 1640 in a XF96 cell culture microplate (Seahorse Bioscience). The service was afforded by BaiHao Biological technology (Liaoning, China). OCR is reported in units of picomoles per minute.

Whole transcriptome sequencing

Total RNA was extracted from gastric tissues of Gan mice using an Eastep Total RNA Extraction Kit (Promega). RNA purity was assessed using a Nanodrop spectrophotometer (NanoDrop, Wilmington, DE) and Agilent 2100 Bioanalyzer (Agilent, Palo Alto, CA). Sequencing was done on an Illumina Genome Analyzer (Illumina, San Diego, CA). The sequencing service and bioinformatics analysis were afforded by the Shanghai Biotechnology Corporation (Shanghai, China). In addition, all the sequence raw data were uploaded in SRA database with the accession number was SRP151505.

mRNA quantification

Total RNA was extracted from gastric tissues and GC cells in different conditions, and the qRT-PCR analyses of TLR2 were performed using SYBR Master Mix (Roche, Basel, Switzerland) on a LightCycler 480 Real Time PCR system (Roche); GAPDH was used as an internal control.

Methylated DNA immunoprecipitation (MeDIP) sequencing

Genomic DNA was extracted from gastric tissues in Gan mice with a DNeasy Kit (TransGen, China). A total of 1.25 µg of genomic DNA were subjected to bisulfite conversion using the EZ DNA Methylation Gold Kit (Zymo Research, Irvine, CA). Approximately, 600 ng of bisulfite-converted DNA was analyzed on an Infinium Analyzer (Illumina). The sequencing service and bioinformatics analysis were afforded by the Shanghai Biotechnology Corporation. In addition, all the sequence raw data were uploaded in SRA database with the accession number SRP151505.

CpG island research

The DNA sequences from –5000 to +1000 bp of TLR2 were predicated to find the potential CpG island using the EMBOSS website (http://www.ebi.ac.uk/Tools/seqstats/emboss_cpgplot/) with the following criteria [i.e. length > 200 bp, observed/expected ratio > 0.60, percentage (C+G) > 50%]. Then, the primers for methylation specific PCR (MSP) were designed using MethPrimer (http://www.urogene.org/cgi-bin/methprimer/methprimer.cgi).

MassARRAY

Genomic DNA was isolated, and bisulfite was converted as mentioned above. The CpG island located in the –169/+332 nt region of the TLR2 promoter was determined using the Sequenom MassARRAY system (Sequenom, San Diego, CA) using the following primers: Forward: 5′-AGGAAGAGAGTTTTAGGAAGGGGTGTAGAGAGATT-3′, Reverse: 5′-CAGTAATACGACTCACTATAGGGAGAAGGCTACTTTCCCTATAATTACCAATCCCA-3′. The above services were provided by the Biomiao Biotechnology Corporation (Beijing).

Methylation specific PCR (MSP)

The bisulfate-converted DNA was amplified by PCR with two sets of methylation-specific primers (TLR2 M-F: 5′-TTCGGGAGAAGT AGGGGTTATAC-3′, M-R: 5′-AAACCTACAAAA TTAAAAAAACGCT-3′, U-F: 5′-TTTTTGGGAGAAGT AGGGGTTATAT-3′ U-R: 5′-AAACCTACAAAATTAAAAAAACACT-3′). The PCR

conditions were as follows: 35 cycles of 94°C for 50 s, 56°C for 50 s and 72°C for 50 s. The resulting PCR products were resolved using 1.5% agarose gel electrophoresis.

Statistical analyses

All statistical analyses were carried out using the SPSS 12.0 software (Chicago, IL) and GraphPad Prism 5.04 (GraphPad Software), unless otherwise indicated. The data are shown as the mean ± SD, and each assay was represented by at least three replicates. The difference between two groups was analyzed using a Student's *t*-test. The survival curve was generated by a log-rank test. Multivariate Cox regression was performed to assess the hazard ratios and 95% CIs of possible independent prognostic factors of GC. *P* < 0.05 was significant.

Results

Suppression effects of GRA on gastric tumorigenesis in Gan mouse

In the Control group, the gastric epithelial mucosa showed dramatic hypertrophy, while HE staining showed atypical hyperplasia, protruded lesions and *in situ* carcinoma, as well as lymphocyte infiltration in the upper stomach. The gastric tumor is similar to Borrmann type I of human GC (Figure 1A). However, in the GRA-treated group, the atypia of cells, abnormity of tissue structure and arrangement of gastric glands were alleviated, and the inflammatory reaction was also reduced (Figure 1B). The incidence of gastric tumors was 66.6% (24/36) in the Control group, while it decreased to 38.9% (14/36) in the GRA-treated group (*P* = 0.008). The average tumor volume was 524.1 ± 56.2 mm³, while it decreased into 305.4 ± 33.6 mm³ in the GRA-treated group (*P* = 0.001) (Figure 1A).

Furthermore, the cell proliferation marker Ki-67 and macrophage marker F4/80 were analyzed using IHC staining. The results showed that Ki-67-labeled cells were found throughout tumor tissues in the Control group, whereas they were mostly limited to the tumor surface in the GRA-treated group (Figure 1C). Heavy macrophage accumulation was found in the gastric tumors of Control mice, whereas tissue macrophages were sparsely scattered in the GRA-treated group (Figure 1D).

TLR2 signaling pathway was a potential target of GRA

To investigate the GRA-regulated genes and pathways systematically, the transcription profiles in the gastric tumor tissues (Tumor), adjacent tissues (Non-tumor) and GRA-treated tumor tissues (GRA-treated Tumor) were analyzed in Gan mouse models using whole transcriptome sequencing. Compared with Non-tumor tissues, 1358 genes were differentially expressed, exhibiting a fold change of ≥2.0 and *q* value of <0.05, of which 949 (70%) were downregulated and 409 (30%) were upregulated in Tumor tissues (Figure 1E). Compared with Tumor tissues, 433 genes were identified as differentially expressed (fold change ≥2.0, *q* value of <0.05), of which 155 (36%) were downregulated and 278 (64%) were upregulated after GRA treatment (Figure 1F). KEGG pathway enrichment analysis showed that TLRs, PPAR and gastric acid secretion signaling pathways were involved in the inhibition effects of GRA on gastric carcinogenesis (Figure 1G). Between TLR families, TLR2 was overexpressed in Tumors in the Control group (fold change = 3.73, *q* value of <0.01) and downregulated in Tumors in the GRA-treated group (fold change = −1.87, *q* value of <0.01) (Figure 1H).

To confirm the transcriptome sequencing results, qRT-PCR was performed to screen the expression levels of TLR2 in paired fresh tumor tissues and adjacent tissues isolated from nine Gan mice; the results showed that TLR2 was indeed higher in

GC tissues than that in adjacent tissues (Figure 1I), and it was suppressed by GRA treatment both in mRNA (Figure 1J) and protein level (Supplementary Figure 1, available at *Carcinogenesis* Online). Further western blot demonstrated that GRA downregulated the TLR2/MyD88 signaling pathway in GC cell line KATOIII (Figure 1K), suggesting that TLR2 was a potential target of GRA.

TLR2 pathway was involved in GC cell proliferation

The RT-PCR and immunoblot results showed that TLR2 had low expression in the immortal gastric epithelial cell GES-1, while it was overexpressed in MKN-1, AGS and aberrantly hyperactive in KATOIII (Figure 2A and B). The TLR2 specific agonist PA-LPS significantly enhanced GC cell viability in MKN-1 with lower TLR2 expression (Figure 2C), while the TLR2-specific blocking reagent CU CPT22 inhibited cell viability in KATOIII with higher TLR2 expression (Figure 2D). Moreover, TLR2 overexpression stimulated the cell growth of MKN-1 in a concentration-dependent manner (Figure 2E), while blocking TLR2 expression decreased the KATOIII growth ability (Figure 2F). Furthermore, the effect of TLR2 on the GC cell cycle was also analyzed, but TLR2 has no significant effect on the cell cycle after PA-LPS and CU CPT22 exposure (data not shown). Further analysis showed that NF-κB and MyD88 are involved in the TLR2 signaling pathway, and Wnt-1, β-catenin and COX-2, which are involved in GC cell proliferation, were stimulated by TLR2 overexpression, while TLR4 was not influenced by PA-LPS stimulation (Figure 2G). In addition, the expressions levels of NF-κB, MyD88, Wnt-1, β-catenin and COX-2 were downregulated when TLR2 was blocked by specific inhibitor CU CPT22, while TLR4 was not changed by and large (Figure 2H).

TLR2 expression was correlated with GC histological grade and poor survival

Using 13 pairs of human gastric tumor tissue (Tumor, T) and adjacent normal tissues (Non-tumor, N), TLR2 was also overexpressed in Tumor on both the mRNA and protein level as that in Gan mice (Figure 3A–C). Moreover, the protein location and expression were determined in 13 paired gastric tissues and 53 cases of gastric tumor tissues using IHC staining. Normal gastric epithelia and stroma were generally negative for TLR2, while TLR2 was localized in the cytoplasm and cell membrane in cancer cells (Figure 3D). Interestingly, in the present study, the relative TLR2 expression level in the tumor tissue of case 1 was much higher than in other cases (Figure 3C), while IHC staining showed that TLR2 was generally negative expressed in gastric epithelia and stroma (Figure 3D). The results suggested that blood corpuscle system cell might be existed in the stroma, and inflammatory cells with TLR2 expression sometimes permeated into the normal tissue. Besides that, the strong staining of TLR2 was characteristic of a high histological grade, whereas the moderate or weak staining of TLR2 was representative of a low histological grade (Figure 3E). Log-rank test showed that the patients with strong TLR2 staining had poor survival (log-rank *P* = 0.022) (Figure 3F). Further multivariate Cox regression test showed that the TLR2 protein expression was an independent prognostic factor. Patients with higher expression level of TLR2 protein had an increased risk of worse prognosis than patients with lower expression level of TLR2 protein (hazard ratio: 474, 95% CI: 1.297–9.306, *P* = 0.013) (Supplementary Table 1, available at *Carcinogenesis* Online).

TLR2 promoted GC cell energy metabolism

To elucidate whether the stimulation effects on the GC cell proliferation of TLR2 were related to mitochondrial energy metabolism, the mitochondrial function, oxidative phosphorylation
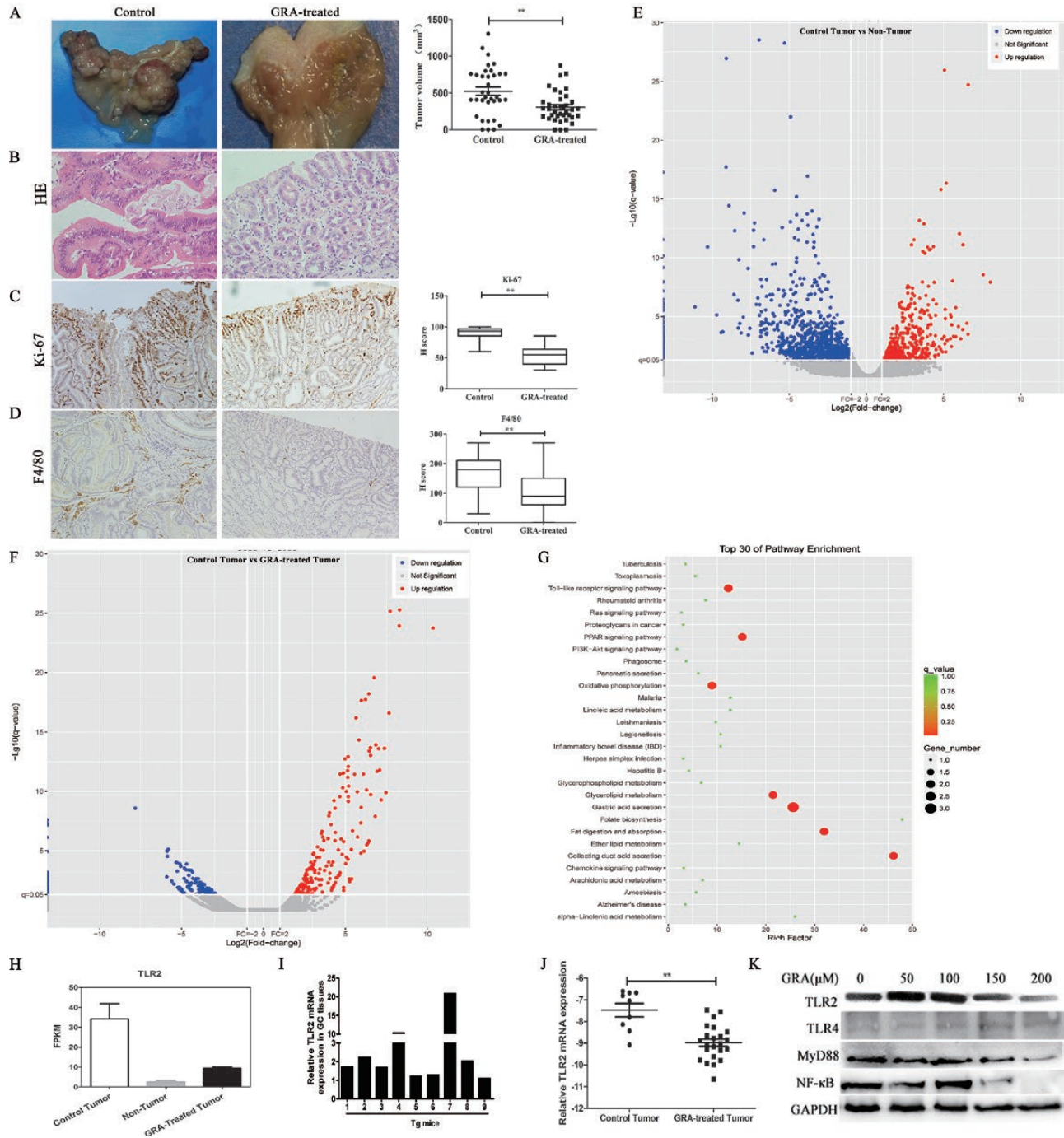
Figure 1. GRA treatment inhibited tumor development and changed gene expression profile in Gan mice. (**A**) Macroscopic photographs with tumor volume. (**B**) HE staining in the Control and GRA-treated group (magnification ×400). (**C**) Ki-67 staining and H score in the Control and GRA-treated group (magnification ×100). (**D**) F4/80 staining and H score in the Control and GRA-treated group (magnification ×100). (**E**) Differentially expressed genes between the Tumor and Non-tumor in Control Gan mouse. Red dots represent upregulated genes in the Tumor, blue dots show those downregulated genes in the Tumor and gray dots indicate that the gene expression did not change significantly. (**F**) Differentially expressed genes between the Control Tumor and GRA-treated Tumor. Red dots represent upregulated genes after GRA treatment, blue dots show those downregulated genes after GRA treatment and gray dots indicate that the gene expression did not change significantly. (**G**) KEGG enrichment analysis of differentially expressed genes between the Control and GRA-treated Tumor tissue. (**H**) FPKM value of TLR2 in the Tumor, Non-tumor of the Control group and the GRA-treated group. (**I**) Relative mRNA expression of TLR2 in 9 pairs of the Tumor and Non-tumor tissue in Gan mice. (**J**) Relative mRNA expression of TLR2 in tumor tissues of the Control group and GRA-treated group. (**K**) Protein expression of the TLR2/MyD88 pathway in KATOIII after GRA treatment. The results are showed as mean ± SD, $n = 3$, *$P < 0.05$; **$P < 0.01$.
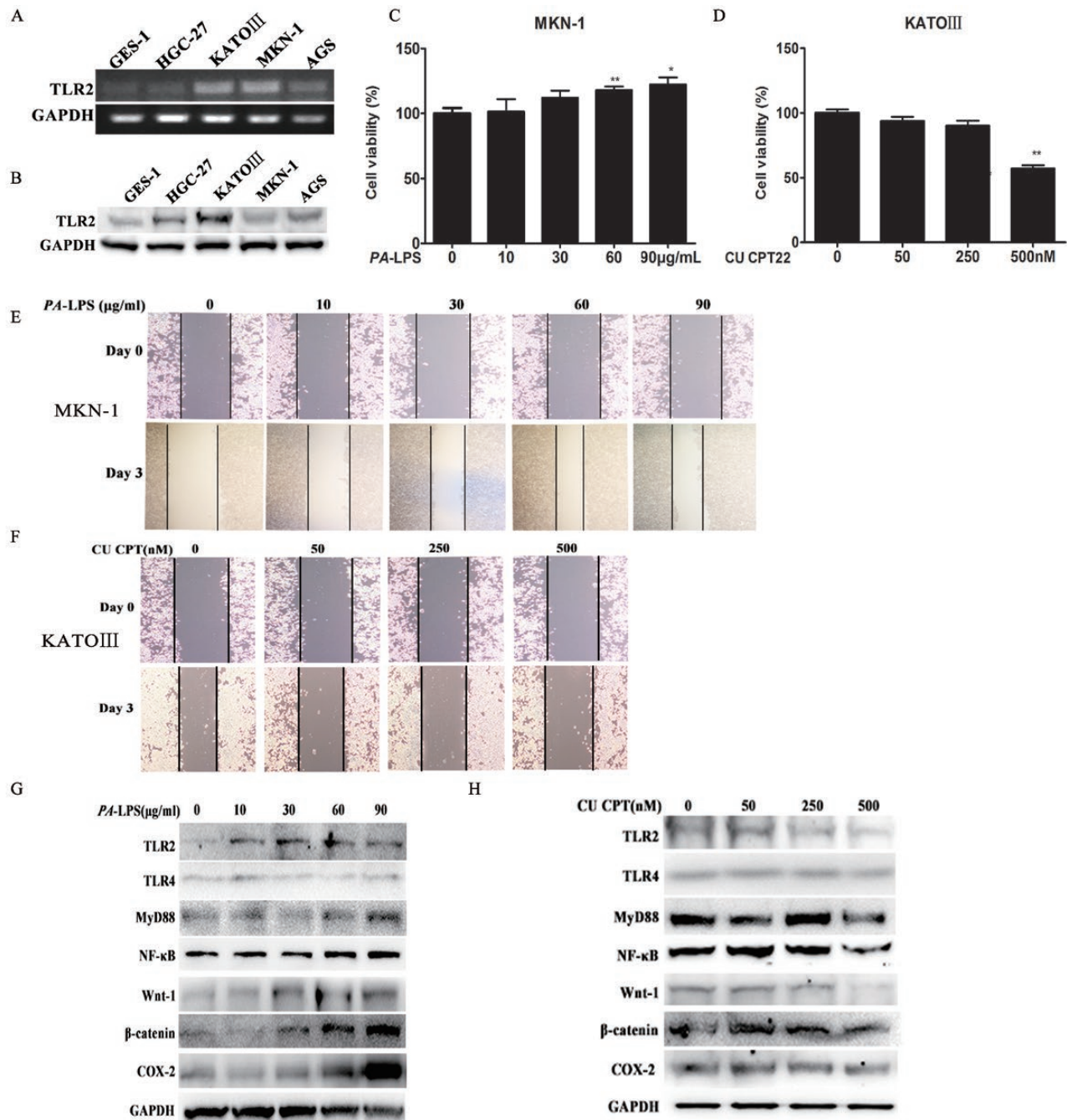
Figure 2. High TLR2 levels facilitated GC cell proliferation and activated growth-responsive signaling pathways. (**A**) mRNA expression of TLR2 in multiple GC cell lines and GES-1. (**B**) Protein expression of TLR2 in multiple GC cell lines and GES-1. (**C**) TLR2 agonist *PA-LPS* stimulated MKN-1 cell viability. (**D**) TLR2 inhibitor CU CPT22 inhibited KATOⅢ cell viability. (**E**) TLR2 agonist *PA-LPS* stimulated MKN-1 cell proliferation. (**F**) TLR2 inhibitor CU CPT22 inhibited KATOⅢ cell proliferation. (**G**) TLR2 agonist *PA-LPS* activated TLR2/MyD88, canonical Wnt/β-catenin, COX-2 signaling pathways. (**H**) TLR2 inhibitor CU CPT22 inhibited TLR2/MyD88, canonical Wnt/β-catenin, COX-2 pathways. The results are showed as means ± SD, *n* = 3, *P < 0.05; **P < 0.01.

(OXPHOS) and ETC were analyzed. Treatment of MKN-1, which had a lower TLR2 expression level, with *PA-LPS* for 24 h induced mitochondrial membrane potential, as well as Ca^{2+} and ROS generation (Figure 4A–C). Besides that, 30 µg/ml *PA-LPS* stimulated the basal OCR to 50.88 ± 7.79 pmol/min per 1×10^4 cells (163.02% of control) (Figure 4D). In addition, the maximal respiration and spare capacity were 61.21 ± 8.44 (199.58% of control) (Figure 4E) and 8.97 ± 1.40 (614.38% of control) pmol/min per 1×10^4 cells (Figure 4F) when MKN-1 were treated with 30 µg/ml *PA-LPS*, respectively. However, 60 and 90 µg/ml

PA-LPS treatment was no longer induce basal OCR, maximal OCR and spare capacity than 30 µg/ml *PA-LPS* treated MKN-1 cells, while the OCR values were still increased compared with Control cells. The no dose-dependency phenomena suggested that lower concentration of *PA-LPS* induced glucose transport and consumption, promoted oxygen and ATP production, while higher concentration of *PA-LPS* treatment might lead to the deficiency of glucose source, and then the oxidative metabolism was reduced at a less magnitude than 10 and 30 µg/ml *PA-LPS* treatment.
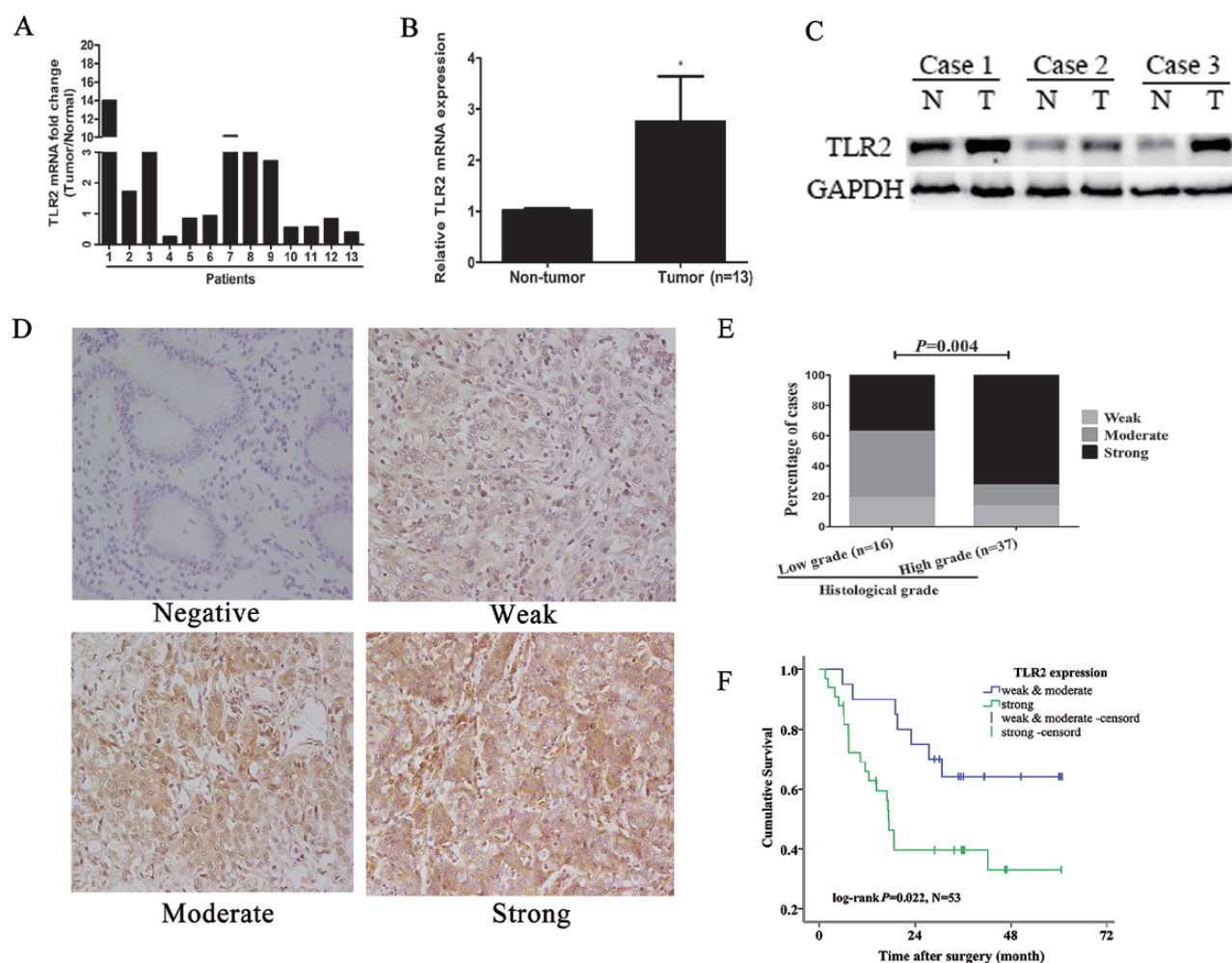
Figure 3. High TLR2 level is associated with differentiation status and poor overall survival in GC patients. (**A**, **B**) Relative mRNA expression of TLR2 in 13 pairs of tumors (T) and matched Non-tumor (N) tissues. (**C**) Protein expression of TLR2 in three typical pairs of tumors (T) and matched Non-tumor (N) tissues. (**D**) Negative, weak, moderate and strong TLR2 stained in Non-tumor and Tumor tissues. (**E**) Expression of TLR2 was checked in 53 GC tissues (low grade $n = 16$; high grade $n = 37$). (**F**) Survival plots for TLR2 expression of GC. *$^{*}P < 0.05$.

Furthermore, KATOIII with higher TLR2 expression was treated by series concentration of CU CPT22. The results showed that blocking TLR2 expression depolarized the inner mitochondrial membrane potential and decreased the intracellular Ca^{2+} content and ROS production in a dose-dependent manner (Figure 4G–I). The basal cellular OCR, maximal respiration and spare respiration in KATOIII were 180.90 ± 17.29, 279.20 ± 12.51 and 106.00 ± 9.07 pmol/min per 1×10^4 (initial cell count) cells, respectively. Treatment with 500 nM CU CPT22 reduced the basal OCR, maximal respiration and spare respiration to 112.80 ± 9.62 pmol/min per 1×10^4 cells (65.13% of control), 145.60 ± 9.03 pmol/min per 1×10^4 cells (52.15% of control) and 42.80 ± 2.21 (40.38% of control) pmol/min per 1×10^4 cells, respectively (Figure 4J–L).

Altogether, these data showed that TLR2 overexpression stimulated mitochondrial function and energy metabolism, while blocking TLR2 expression caused mitochondrial membrane potential, Ca^{2+} and ROS loss, as well as inhibited OXPHOS and ETC.

TLR2 signaling is required for the inhibition effects of GRA on gastric tumorigenesis and energy metabolism

To elucidate whether TLR2 signaling was required for the inhibitory effects of GRA, MKN-1, which has low expression of TLR2, was

pretreated with 0–200 μM GRA for 2 h and then was treated with 60 μg/ml PA-LPS for 24 h. MTT assay, wound healing and colony formation showed that 60 μg/ml PA-LPS promoted gastric tumor cell proliferation, while 200 μM GRA pretreatment inhibited cell viability and propagation (Figure 5A–C). In addition, 60 μg/ml PA-LPS stimulated mitochondrial membrane potential, Ca^{2+} level and ROS generation, while 100–200 μM GRA pretreatment impeded the increase of mitochondrial membrane potential and ROS generation (Figure 5D and F) but has no effect on the Ca^{2+} level (Figure 5E).

Then, the analysis of energy metabolism showed that 60 μg/ml PA-LPS stimulated the basal OCR, maximal respiration and spare capacity, while GRA pretreatment hindered energy metabolism and ATP production (Figure 5G–I). In addition, the expression levels of TLR2, NF-κB, MyD88 and Wnt-1 were stimulated by 60 μg/ml PA-LPS and downregulated by the GRA pretreatment in MKN-1 cell, while TLR4 was not influenced by PA-LPS or GRA treatment (Figure 5J).

TLR2 expression was methylation-regulated by GRA in promoter region

In addition to whole transcriptome sequencing, the methylome profiles in the Tumor tissues (Tumor), adjacent tissues (Non-tumor) and GRA-treated tumor tissue (GRA-treated Tumor) were
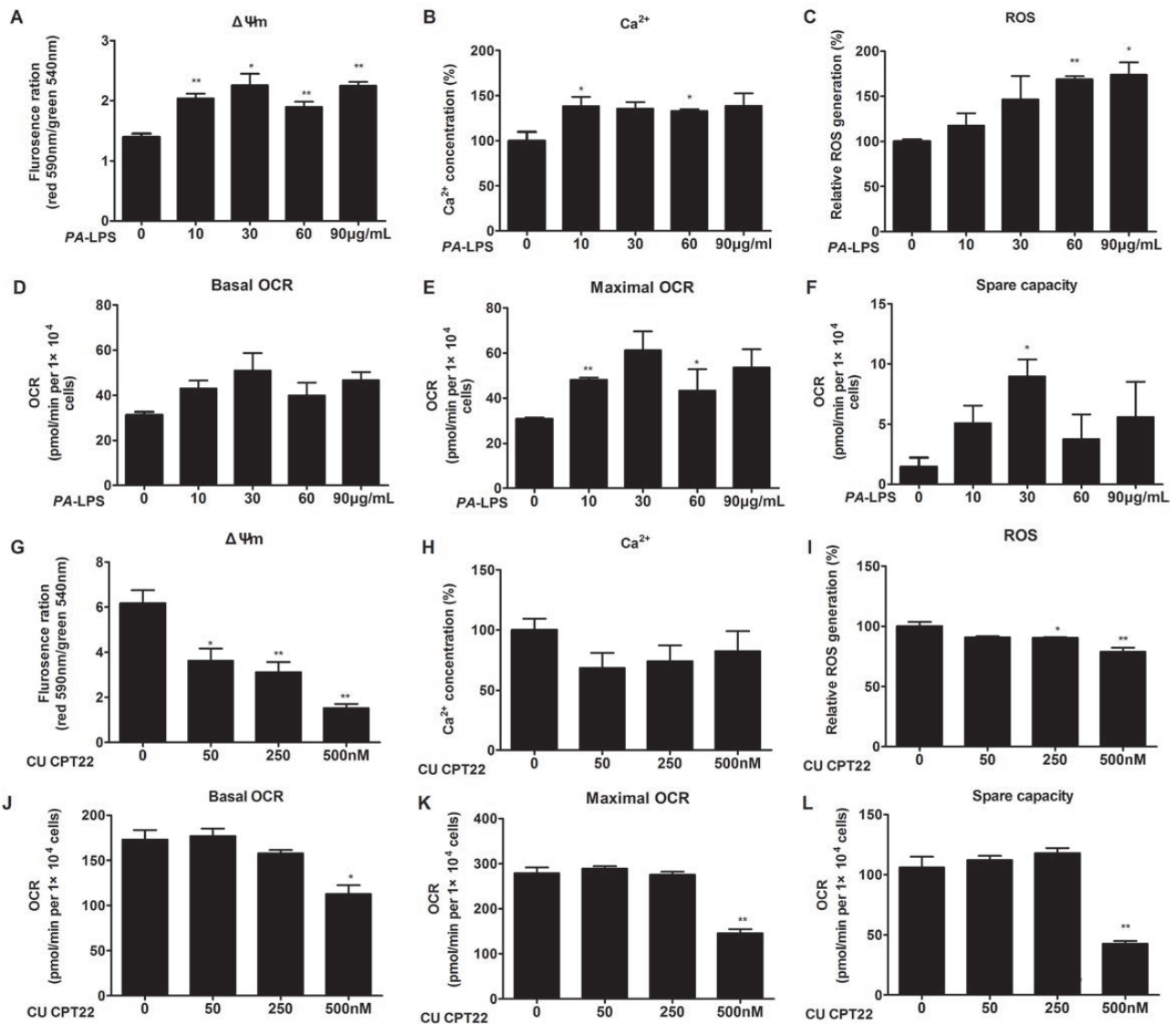
Figure 4. TLR2 is associated with mitochondrial functions and bioenergetics. (**A–F**) TLR2 agonist *PA*-LPS activated mitochondrial membrane potential, Ca^{2+} level, ROS production, basal OCR, maximal OCR and spare capacity. (**G–L**) TLR2 inhibitor CU CPT22 decreased mitochondrial membrane potential, Ca^{2+} level, ROS production, basal OCR, maximal OCR and spare capacity. Results are showed as mean ± SD, $n = 3$, *, $P < 0.05$; **$P < 0.01$.

also analyzed using MeDIP sequencing. Compared with the Non-tumor, 106 445 differential methylation regions were identified, of which 91 039 (86%) were hypermethylated and 15 406 (14%) were hypomethylated in the Tumor. Compared with the Tumor, 62 879 differential methylation regions were identified, of which 16 436 (26%) were hypermethylated and 46 443 (74%) were hypomethylated in GRA-treated Tumor.

Considering the regulation pattern between the methylation status with gene expression, comprehensive data of the whole transcriptome and the methylome in different groups were analyzed. As Figure 6A shows, compared with the Non-tumor, 56 genes were overexpressed in Tumor with hypomethylation in the promoter, and 100 genes were downregulated in the Tumor with hypermethylation in the promoter. Compared with the Tumor, 186 genes were lowly expressed with hypermethylation in GRA-treated group, and 77 genes had high expression with hypomethylation in the GRA-treated group (Figure 6B).

As suggested by MeDIP sequencing, TLR2 was downregulated by GRA treatment with hypermethylation in its promoter. MassARRAY and methylation-specific PCR were used to investigate the potential methylation status of the promoter region. One CpG island was found in the promoter of TLR2 (−5000 to +1000 bp) (length = 924) (Figure 6C). Then, 502 bp from −169 to +332 bp covers 27 CG sites (Figure 6D) was amplified, and MassARRAY showed that CpG sites 5 (CpG position 74) and CpG sites 35 (CpG position 345) differed in their methylation level, and GRA increased the methylation levels of CpG sites 5 and 35 (Figure 6E). MSP results also showed that GRA increased the methylation level and decreased the unmethylation level of TLR2 methylation (Figure 6F and G). Based on these data, we proposed that the increase of the DNA methylation level in the promoter region of the gene TLR2, particularly the CpG 5 or CpG 35 sites, possibly repressed TLR2 expression after GRA treatment.
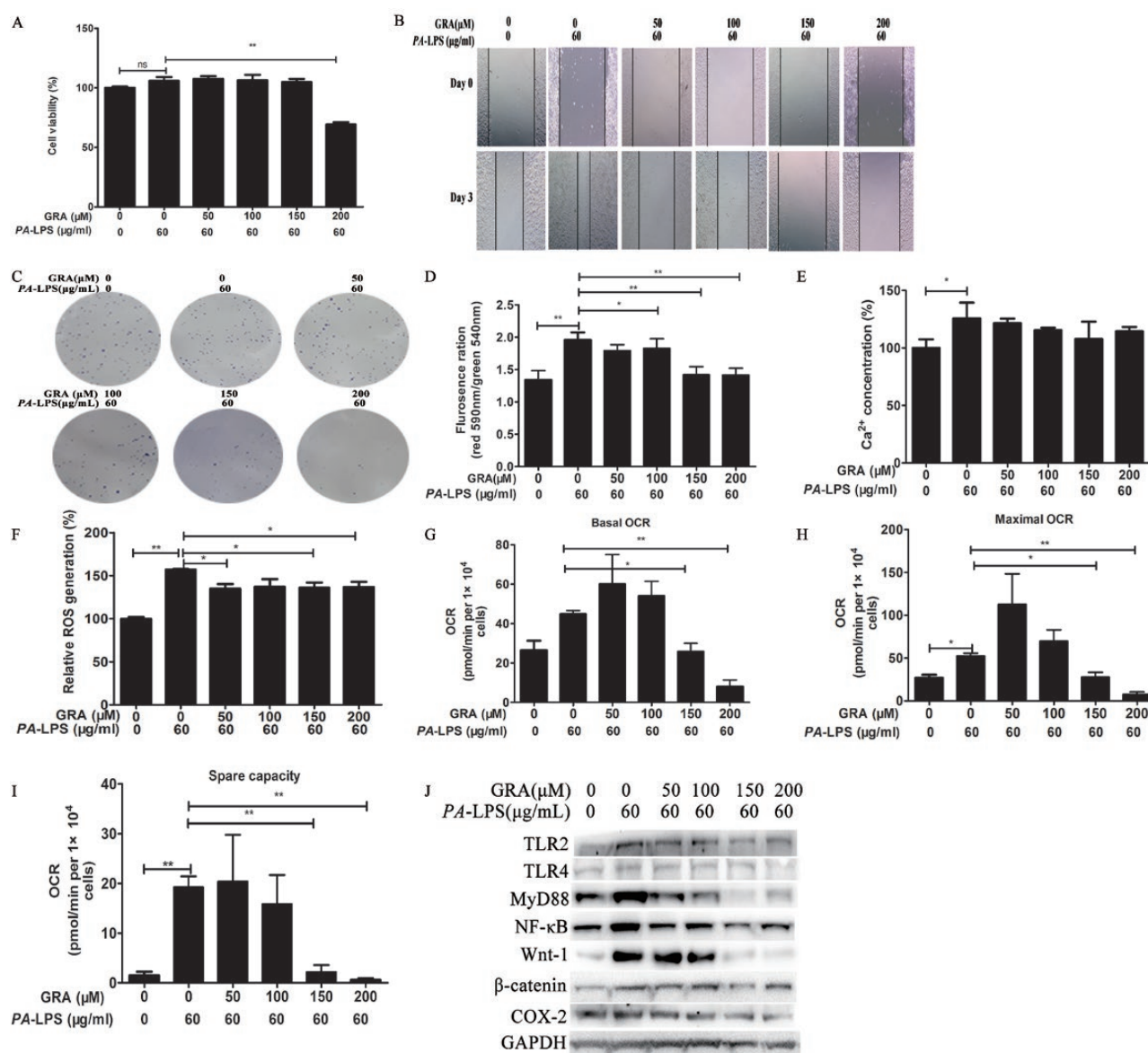
Figure 5. GRA inhibited GC cell proliferation, mitochondrial function and energy metabolism through TLR2 signaling pathway. The cells were pretreated with serial concentration of GRA for 2 h and then stimulated by PA-LPS for 24 h. (**A**) Cell viability. (**B**) Wound healing. (**C**) Colony formation. (**D**) Mitochondrial membrane potential. (**E**) Ca^{2+} level. (**F**) ROS production. (**G**) Basal OCR. (**H**) Maximal OCR. (**I**) Spare capacity. (**J**) GRA downregulated TLR2-activated canonical Wnt/β-catenin and COX-2 pathways. The results are showed as mean ± SD, $n = 3$, *, $P < 0.05$; **$P < 0.01$.

Discussion

The increasing number and changing patterns of cancer worldwide emphasized the cancer prevention as a part of precision medicine (20). Chemoprevention entails the use of natural phytochemicals to prevent gastritis and GC development (21). 18β-GRA is a major active compound of licorice and showed anti-inflammatory and preventative tumor effects on various models (3,4,6). The Gan mice model used in this study developed inflammation-related, glandular-type tumors caused by the simultaneous activation of the Wnt and COX-2/PGE2 pathways, which recapitulated glandular-type human GC development (16). Current results showed that GRA pretreatment inhibited GC cell proliferation, impeded mitochondrial function and energy metabolism, and regulated genetic expression and epigenetic

modifications, suggesting that GRA will be an effective preventive compound for gastric carcinogenesis.

TLR2 mRNA and protein expression levels were elevated in GC patient tumors, Gan mice models and multiple GC cell lines. Furthermore, elevated TLR2 expression was associated with GC differential grades and predicated poor survival. These results suggested that TLR2 was a potential therapeutic target to prevent and treat gastric tumorigenesis. Notably, the treatment of GC cells with a TLR2-specific inhibitor CU CPT22 and genetic targeting of TLR2 in the gp130F/F GC mouse model dramatically suppressed gastric tumor cell growth and carcinogenesis (22). C16H15NO4 (C29) and its derivative ortho-vanillin (o-vanillin) were identified as a potential TLR2 inhibitor, and o-vanillin pretreatment of mice reduced TLR2-induced inflammation (23). GRA impeded TLR2-activated mitochondrial energy metabolism,
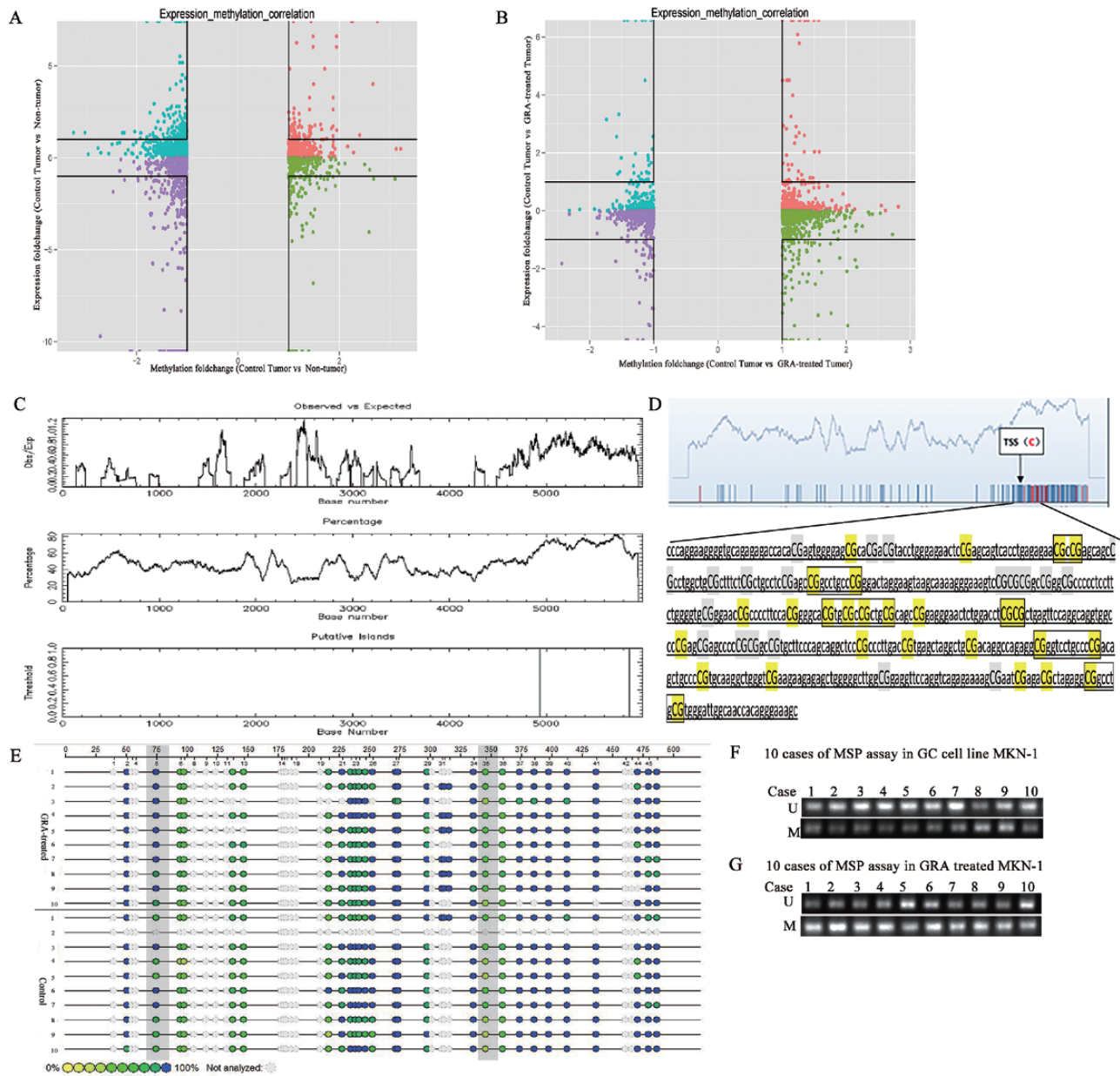
Figure 6. GRA downregulated TLR2 expression through hypermethylation in its promoter. (**A**) Combination analysis of whole transcriptome and MeDIP sequencing showed that genes might be related to tumorigenesis through methylation regulation. Cyan dots represent upregulated genes with hypomethylation in the Tumor, red dots represent upregulated genes with hypermethylation in the Tumor, violet dots represent downregulated genes with hypomethylation in the Tumor, green dots represent downregulated genes with hypermethylation in the Tumor. (**B**) Combination analysis of the whole transcriptome and MeDIP sequencing showed that genes regulated by GRA treatment might be related with methylation status. Cyan dots represent upregulated genes with hypomethylation after GRA treatment, red dots represent upregulated genes with hypermethylation after GRA treatment, violet dots represent downregulated genes with hypomethylation after GRA treatment, green dots represent downregulated genes with hypermethylation after GRA treatment. (**C**) A CpG island was present in the promoter region of TLR2. (**D**) MassARRAY and MSP analysis region in the promoter of TLR2. (**E**) MassARRAY assays in 10 cases of control and GRA-treated MKN-1. (**F**) MSP assay in MKN-1. (**G**) MSP assay in GRA-treated MKN-1.

GC cell proliferation and tumorigenesis in our study, suggesting that GRA could be an ideal candidate chemopreventive agent as a new potential TLR2 inhibitor.

During the generation of the inflammatory microenvironment, stemness and GC tumorigenesis, the interplay of the COX-2/PGE2 and TLR2/MyD88 pathway was required (24). A pathway analysis of human GC shows that both the COX-2 pathway and TLR2/MyD88 signaling are significantly activated in tubular-type GC (25). In cancer tissues, macrophages infiltrate and are activated by the induction of the COX-2/PGE2 pathway, which further induces transcription factors NF-κB and the cytokine signaling pathway (16). TLR2 stimulation in gastric epithelial cells did not promote the infiltration or activation of inflammatory cells, and both the genetic and therapeutic targeting of TLR2 cannot inhibit gastric inflammation in Tye's study (8). However, Rakoff-Nahoum *et al.* (26) showed that the disruption of *Myd88* gene in *Apc*[Min] mice suppressed the production of COX-2 and other cytokines, and TLR/MyD88 signaling prompted spontaneous

intestinal tumorigenesis through induction of COX-2/PGE2 pathway. In addition, Katoh et al. (27) also indicated gastric epithelia cells recognized LPS by TLR2 and then activated Wnt-β-catenin-T-cell factor/lymphoid enhancer factor signaling cascade to promote gastric tumorigenesis. In our present study, TLR2 activation induced Wnt-1, β-catenin and COX-2 expression, while TLR2 inactivation inhibited Wnt/β-catenin and COX-2 expressions, suggesting that the crosstalk between TLR2/MyD88, Wnt/β-catenin and COX-2/PGE2 pathway existed in the procedure of gastric tumorigenesis. Notably, GRA treatment inhibited inflammation infiltration and downregulated F4/80 expression, in addition, COX-2 was decreased more conspicuously after GRA treatment than specific TLR2 inhibitor CU CPT22 treatment, suggesting that GRA could inhibit COX-2 expression not only directly through COX-2/PGE2 pathway but also indirectly through TLR2/MyD88 pathway. GRA treatment not only downregulated TLR2/MyD88 but also COX-2/PGE2 pathway, implying GRA had the immense potential to inhibit inflammation and GC tumorigenesis.

Many vital cellular parameters, including the regulation of energy production, control of cytosolic Ca^{2+} levels, modulation of redox status, ROS generation and initiation of apoptosis, are involved in carcinogenesis. Cancer cells are metabolically active and consume more cellular energy than normal cells. Although cancer cells mainly rely on aerobic glycolysis and increased glucose metabolism, a feature known as the Warburg effect, malignant tumor cells may utilize other kinds of mitochondrial bioenergetic metabolism, such as fatty acid oxidation and cholesterol synthesis, to meet their requirements for synthesizing nucleic acids, lipids and proteins during their growth and metastasis (28). TLR4 induced cytochrome c oxidase upregulation, altered mitochondrial membrane potential, COX activity and ATP production in murine macrophages (29). TLR2 activation by Pam3cys leads to the robust production of both cellular H_2O_2 and mitochondrial O^{2-} but had no effect on mitochondrial ΔΨm and ATP production in a mouse model of polymicrobial sepsis (30). TLRs activation promoted the association of the glycolytic enzyme HK-II with mitochondrial, increased glycolytic flux via the kinases TBK1, IKKε and Akt (31). Bauerfeld et al. (29) identified that TLR4 phosphorylated the PI3K/AKT pathway, increased the expression of mitochondrial transcriptor A (T-fam) and cytochrome c oxidase (COX, complex IV) and activated ATP production. In addition, TLR2 activated Wnt/β-catenin pathway in our study, suggesting that TLR2 promoted OXPHOS, ETC and ATP production through the Wnt/β-catenin pathway.

Conventionally, high levels of ROS are thought to be cytotoxic and mutagenic, rendering the cells oxidatively stressed, impairing membrane proteins, leading to mitochondrial dysfunction, altering mitochondrial bioenergetics and inducing cell death, apoptosis and senescence (32,33). Recently, high levels of ROS have been shown to act as a secondary messenger, controlling various signaling cascades and leading to the sustained proliferation and metastasis of cancer cells (34). H.pylori-infected gastric epithelial cells generated ROS and promoted gastric carcinogenesis through ROS-HIF1α axis (35). Overexpression of TLR2 stimulated ROS production in our study, and Yuan et al. (12) also demonstrated the activation of TLR4-induced ROS generation in GC; excessive ROS production also activates the TLR4/MyD88 signaling (36), suggesting that positive feedback might exist between ROS generation and the TLR signaling pathway.

Epigenetic alterations are early events during carcinogenesis (37), and phytochemicals have shown the potential to modulate major epigenetic pathways (38). In this study, TLR2 is highly expressed in Gan GC and various GC cell lines, and GRA treatment hypermethylated the TLR2 promoter and downregulated

TLR2 expression. During the inflammatory response against infection, TLR2 was aberrantly expressed with enhanced DNA demethylation (39). Treatment of the cells with 5-azacytidine decreased promoter methylation and increased endogenous expression of TLR2, suggesting that TLR2 expression is epigenetically regulated by CpG methylation (40). In addition to DNA methylation regulation, GRA treatment also has epigenetic effects through miRNA and histone modification. miRNA assays showed that the tumor suppressor miR-149-3p targeting Wnt-1 was upregulated by GRA in our previous study (3). Molecular docking and surface plasmon resonance assays identified that GRA could directly bind to histone deacetylases (HDAC2) and attenuate its activity (41). Therefore, GRA showed the ability to reverse the epigenetic changes responsible for the risk of GCs. Recently, dietary compounds capable of maintaining the epigenetic regulation balance have appeared as an attractive preventive and therapeutic approach against human cancer, and our results implied that the hypermethylation of TLR2 by GRA can provide an alternative epigenetic therapy for GC.

Supplementary material

Supplementary data can be found at *Carcinogenesis* online.

Funding

References

1. Ferlay, J. et al. (2015) Cancer incidence and mortality worldwide: sources, methods and major patterns in GLOBOCAN 2012. Int. J. Cancer, 136, E359–E386.
2. Chen, W. et al. (2017) Cancer incidence and mortality in China, 2013. Cancer Lett., 401, 63–71.
3. Cao, D. et al. (2016) 18β-glycyrrhetinic acid suppresses gastric cancer by activation of miR-149-3p-Wnt-1 signaling. Oncotarget, 7, 71960–71973.
4. Cao, D.H. et al. (2016) The protective effects of 18β-glycyrrhetinic acid on *Helicobacter pylori*-infected gastric mucosa in Mongolian gerbils. Biomed Res. Int, 2016, 1–8.
5. Cai, H. et al. (2018) 18β-glycyrrhetinic acid inhibits migration and invasion of human gastric cancer cells via the ROS/PKC-α/ERK pathway. J. Nat. Med., 72, 252–259.
6. Cao, D. et al. (2018) The protective effects of 18β-glycyrrhetinic acid against inflammation microenvironment in gastric tumorigenesis targeting PGE2-EP2 receptor-mediated arachidonic acid pathway. Eur. J. Inflam., 16, 1–7.
7. Kim, S. et al. (2009) Carcinoma-produced factors activate myeloid cells through TLR2 to stimulate metastasis. Nature, 457, 102–106.
8. Tye, H. et al. (2012) STAT3-driven upregulation of TLR2 promotes gastric tumorigenesis independent of tumor inflammation. Cancer Cell, 22, 466–478.
9. West, A.C. et al. (2017) Identification of a TLR2-regulated gene signature associated with tumor cell growth in gastric cancer. Oncogene, 36, 5134–5144.
10. Hanahan, D. et al. (2011) Hallmarks of cancer: the next generation. Cell, 144, 646–674.
11. Tohme, S. et al. (2017) Hypoxia mediates mitochondrial biogenesis in hepatocellular carcinoma to promote tumor growth through HMGB1 and TLR9 interaction. Hepatology, 66, 182–197.
12. Yuan, X. et al. (2013) Activation of TLR4 signaling promotes gastric cancer progression by inducing mitochondrial ROS production. Cell Death Dis., 4, e794.

13. Sehrawat, A. *et al.* (2017) Mitochondrial dysfunction in cancer chemo-prevention by phytochemicals from dietary and medicinal plants. Semin. Cancer Biol., 47, 147–153.

14. Wang, D. *et al.* (2014) 18beta-glycyrrhetinic acid induces apoptosis in pituitary adenoma cells via ROS/MAPKs-mediated pathway. J. Neurooncol., 116, 221–230.

15. Capes-Davis, A. *et al.* (2013) Match criteria for human cell line authentication: where do we draw the line? Int. J. Cancer, 132, 2510–2519.

16. Oshima, H. *et al.* (2006) Carcinogenesis in mouse stomach by simultaneous activation of the Wnt signaling and prostaglandin E2 pathway. Gastroenterology, 131, 1086–1095.

17. Cao, D. *et al.* (2015) Canolol inhibits gastric tumors initiation and progression through COX-2/PGE2 pathway in K19-C2mE transgenic mice. PLoS One, 10, e0120938.

18. Paeng, S.H. *et al.* (2015) YCG063 inhibits *Pseudomonas aeruginosa* LPS-induced inflammation in human retinal pigment epithelial cells through the TLR2-mediated AKT/NF-κB pathway and ROS-independent pathways. Int. J. Mol. Med., 36, 808–816.

19. Ghonime, M.G. *et al.* (2015) Inflammasome priming is similar for *Francisella* species that differentially induce inflammasome activation. PLoS One, 10, e0127278.

20. Stewart, B.W. *et al.* (2016) Cancer prevention as part of precision medicine: 'plenty to be done'. Carcinogenesis, 37, 2–9.

21. Cao, X. *et al.* (2008) 4-Vinyl-2,6-dimethoxyphenol (canolol) suppresses oxidative stress and gastric carcinogenesis in *Helicobacter pylori*-infected carcinogen-treated Mongolian gerbils. Int. J. Cancer, 122, 1445–1454.

22. Kennedy, C.L. *et al.* (2014) Differential role of MyD88 and Mal/TIRAP in TLR2-mediated gastric tumourigenesis. Oncogene, 33, 2540–2546.

23. Mistry, P. *et al.* (2015) Inhibition of TLR2 signaling by small molecule inhibitors targeting a pocket within the TLR2 TIR domain. Proc. Natl. Acad. Sci. USA, 112, 5455–5460.

24. Echizen, K. *et al.* (2018) The inflammatory microenvironment that promotes gastrointestinal cancer development and invasion. Adv. Biol. Regul., 68, 39–45.

25. Echizen, K. *et al.* (2016) Inflammation in gastric cancer: interplay of the COX-2/prostaglandin E2 and Toll-like receptor/MyD88 pathways. Cancer Sci., 107, 391–397.

26. Rakoff-Nahoum, S. *et al.* (2007) Regulation of spontaneous intestinal tumorigenesis through the adaptor protein MyD88. Science, 317, 124–127.

27. Katoh, M. (2007) Dysregulation of stem cell signaling network due to germline mutation, SNP, *Helicobacter pylori* infection, epigenetic change and genetic alteration in gastric cancer. Cancer Biol. Ther., 6, 832–839.

28. Gupta, S. *et al.* (2017) Metabolic cooperation and competition in the tumor microenvironment: implications for therapy. Front. Oncol., 7, 68.

29. Bauerfeld, C.P. *et al.* (2012) TLR4-mediated AKT activation is MyD88/TRIF dependent and critical for induction of oxidative phosphorylation and mitochondrial transcription factor A in murine macrophages. J. Immunol., 188, 2847–2857.

30. Gong, Y. *et al.* (2014) Importance of Toll-like receptor 2 in mitochondrial dysfunction during polymicrobial sepsis. Anesthesiology, 121, 1236–1247.

31. Everts, B. *et al.* (2014) TLR-driven early glycolytic reprogramming via the kinases TBK1-IKKε supports the anabolic demands of dendritic cell activation. Nat. Immunol., 15, 323–332.

32. Idelchik, M.D.P.S. *et al.* (2017) Mitochondrial ROS control of cancer. Semin. Cancer Biol., 47, 57–66.

33. Wakiyama, K. *et al.* (2017) Low-dose YC-1 combined with glucose and insulin selectively induces apoptosis in hypoxic gastric carcinoma cells by inhibiting anaerobic glycolysis. Sci. Rep., 7, 12653.

34. Kumar, B. *et al.* (2008) Oxidative stress is inherent in prostate cancer cells and is required for aggressive phenotype. Cancer Res., 68, 1777–1785.

35. Wen, J. *et al.* (2018) *Helicobacter pylori* infection promotes Aquaporin 3 expression via the ROS-HIF-1α-AQP3-ROS loop in stomach mucosa: a potential novel mechanism for cancer pathogenesis. Oncogene, 37, 3549–3561.

36. Liu, Z.W. *et al.* (2015) Matrine pretreatment improves cardiac function in rats with diabetic cardiomyopathy via suppressing ROS/TLR-4 signaling pathway. Acta Pharmacol. Sin., 36, 323–333.

37. Takeshima, H. *et al.* (2015) Identification of coexistence of DNA methylation and H3K27me3 specifically in cancer cells as a promising target for epigenetic therapy. Carcinogenesis, 36, 192–201.

38. Shukla, S. *et al.* (2014) Epigenetic regulation by selected dietary phytochemicals in cancer chemoprevention. Cancer Lett., 355, 9–17.

39. Shuto, T. (2013) [Regulation of expression, function, and inflammatory responses of innate immune receptor Toll-like receptor-2 (TLR2) during inflammatory responses against infection]. Yakugaku Zasshi, 133, 1401–1409.

40. Shuto, T. *et al.* (2006) Promoter hypomethylation of Toll-like receptor-2 gene is associated with increased proinflammatory response toward bacterial peptidoglycan in cystic fibrosis bronchial epithelial cells. FASEB J., 20, 782–784.

41. Ma, T. *et al.* (2016) A potential adjuvant chemotherapeutics, 18β-glycyrrhetinic acid, inhibits renal tubular epithelial cells apoptosis via enhancing BMP-7 epigenetically through targeting HDAC2. Sci. Rep., 6, 25396.